Journal of Modern Science and Technology
Vol. 2. No. 2. September 2014 Issue. Pp.113-126

Investigation of Drag Analysis of Four Different Profiles Tested at Subsonic Wind Tunnel

Munzarin Morshed[1], Shehab Bin Sayeed[2], Syed Abdullah Al Mamun[2] and GM Jahangir Alam[3]

The amount of drag produced significantly depends on shape. This investigation deals with the drag analysis of four different profiles, which are cylinder, sphere, symmetrical aerofoil (NACA 0015) and cambered aerofoil (NACA 4415) objects of same volume. The four different types of objected has been tested at a sub-sonic wind tunnel and experimental data has been obtained at different Reynolds's Number and angle of attack. The two aerofoils (symmetrical NACA 0015 and cambered NACA 4415) have been tested from -3˚ to 18˚ angles of attack with 3˚ steps and spherical ball, cylindrical shaped profiles have been tested from 0˚ to 180˚ angles with 10˚ steps at different Reynolds Number. All the four objects have been tested at 10m/s, 15m/s, 20m/s, 25m/s and 30m/s velocities respectively. The cambered aerofoil has provided the least drag and the spherical ball has provided the maximum drag among all the profiles. At last, some conclusions have been drawn after analyzing the drag of all the profiles at different Reynolds's Number.

Field of Research: Mechanical Engineering

Keywords: Wind Tunnel, Drag Coefficient, Aerofoil, Reynolds Number.

1. Introduction

This investigation documents the aerodynamic characteristics of four profiles, as cylinder, sphere, symmetrical aerofoil (NACA 0015) and cambered aerofoil (NACA 4415) objects of same volume. These have been analyzed in a comparison study dealing with their aerodynamic properties, tested at a sub-sonic wind tunnel and obtained experimental data at different Reynolds's Number and angle of attack. Improvement of our understanding of aerodynamic drag force experienced by the different shape of objects, are important for the design strategies of turbine blades, aerodynamic body, aero plane, high architectural structure etc. This performance dataset may be helpful in validating aerodynamic force prediction codes in support of such design activities. This paper explains the details the variation of drag coefficient with Reynolds number for symmetric aerofoil NACA 0015, cambered aerofoil NACA 4415, cylinder and sphere fabricated by wood.

This paper also explicates the cogency of the experimental investigation corresponding with the theoretical aerodynamic characteristics. In both Aerospace and Automotive industry, aerodynamics plays a critical role in vehicle design. Shapes and designs are optimized to obtain the lowest drag possible.

---

[1]Researcher, Masters Student in Oil and Gas Engineering, Memorial University of Newfoundland, Canada, Email: munzarin.mahee@gmail.com
[2]Researcher, Department of Mechanical Engineering, Military Institute of Science and Technology (MIST), Dhaka, Bangladesh.
[3]Instructor Class A, Department of Mechanical Engineering, MIST, Dhaka, Bangladesh, Email: jahangiralam105@yahoo.com

2.1 Aerodynamic Forces Experienced by an Aircraft

Aerodynamic forces are experienced when an aerofoil placed in the uniform flow of an air stream which is created by virtue of the relative motion. The resultant of these aerodynamic forces can be resolved into two force components, parallel and perpendicular to the main flow direction. The vertical force exerted by the fluid on the body is termed as *lift* force, and the component of the total aerodynamics reaction which is parallel and opposite to the flight path of aircraft is called the *drag* force

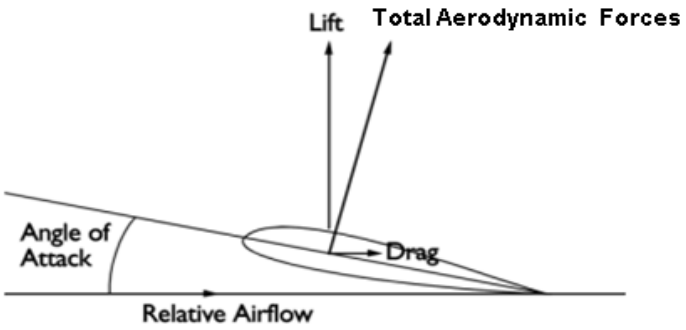

Figure 2.1: Aerodynamic Forces on a Typical Aerofoil

Lift and drag force data are usually expressed in dimensionless terms by using **lift coefficient** and **drag coefficient**. The lift coefficient is defined as:

$$C_L = \frac{L}{\frac{1}{2}\rho V^2 S.}$$

Here, L is the Lift produced, ρ is the Density of air, V is the Velocity of the body and S is the Area of the body or aerofoil. Again, the drag coefficient is defined as:

$$C_D = \frac{D}{\frac{1}{2}\rho V^2 S.}$$; Where D id the drag force.

2.2 Lift and Drag of a Circular Cylinder

The lift generated by an airplane wing or a curving baseball is quite familiar. A simple rotating cylinder also creates lift. Kutta-Joukowski lift theorem for a cylinder is used to explain the situation. [Clancy 1975]

Drag force varies with Reynolds number. Theoretically in subsonic level of air speed the curve is a straight line in the Figure 1 [Scruton and Rogers, 1971]. As the investigation is done at 10 m/s to 25 m/s air speed, so in this range the graph shows a straight line.

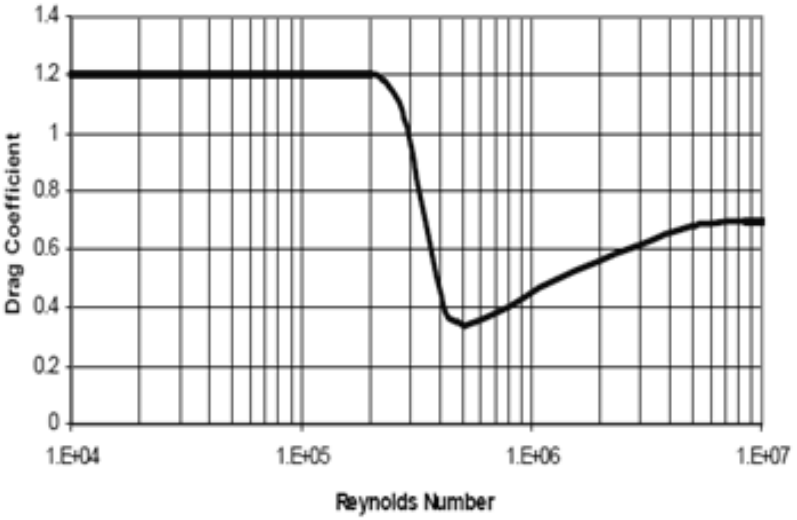

Figure 1: Drag Coefficient vs. R_e number for a circular cylinder, Scruton and Rogers (1971)

2.3 Lift and Drag of a Sphere

Necessity of Creation of lift is to turn a flow of air. Where there is less amount of drag, more lift is produced. The airfoil of a wing turns a flow, and so does a rotating cylinder. A spinning ball or sphere also turns a flow and generates an aerodynamic lift and drag force.

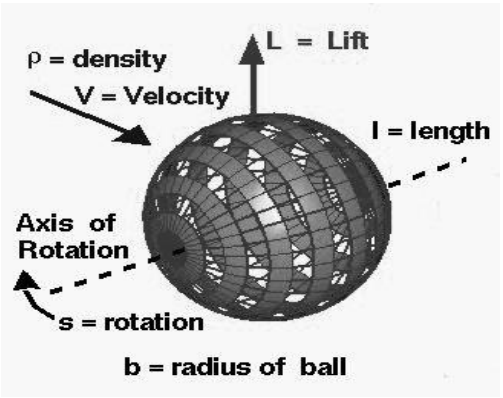

Figure 2: A Circular Sphere

The variation of drag coefficient with Reynolds number is seen in the Figure 3. The curve is a parabolic curve in ideal case.

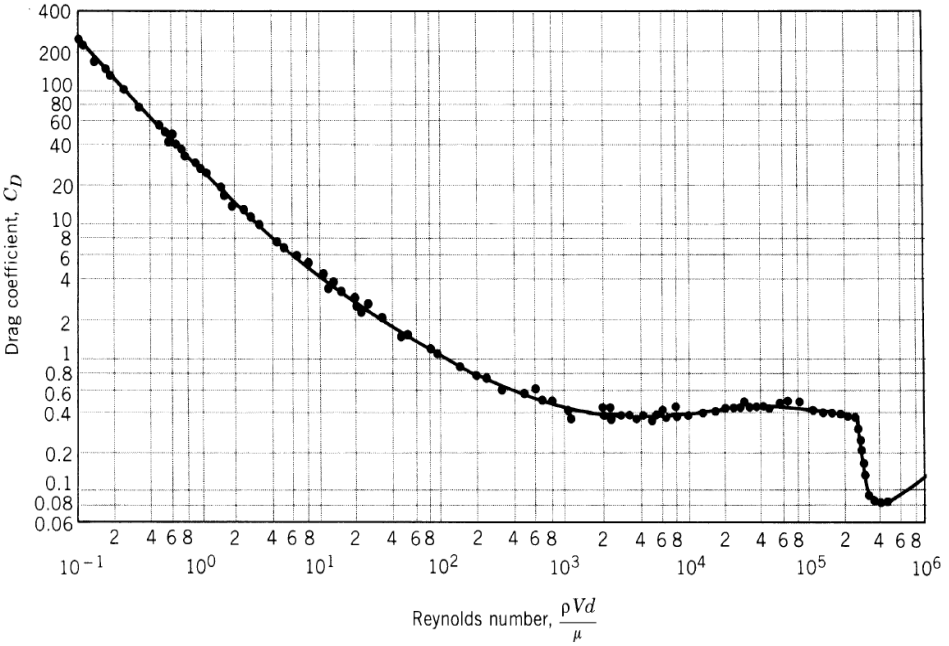

Figure 3: Variation of Drag Coefficient with Reynolds Number for a Sphere in Ideal Case (http://www.grc.nasa.gov/WWW/k-12/airplane/dragsphere.html)

If a cylinder or sphere with roughed surface in a stream of air is rotating, the rough surface of the cylinder, through friction, causes the air in the vicinity to travel round with it, thus inducing circulation, which gives rise to lift. This phenomenon is known as the Magnus effect. For example this effect is responsible for the swing of a sliced golf tennis ball.

2.4 Aerofoil Terminology

The cross-sectional shape obtained by the intersection of an aircraft wing with the perpendicular plane is called an aerofoil [Anderson 1991 and Glauert 1926]. The major design feature of an aerofoil is the mean camber line. Mean Camber Line is the line drawn halfway between upper and lower surfaces. The most forward and rearward points of the mean camber line are the leading and trailing edges respectively. Straight line connecting leading edge and trailing edge is called Chord Line of an aerofoil and length of chord line in the aerofoil is called Chord Length. Maximum distance between mean camber line and chord line is Maximum Camber and Maximum Thickness is the distance between upper and lower surfaces of an aerofoil. The most significant terminology of aerofoil is the angle of attack. It is the angle between the wing chord line and the direction of the flight path. Lift and drag of an aircraft mainly depends on it.

The measure of sharpness of leading edge of aerofoil is the Leading edge radius. And the aspect ratio of a wing is the span (b) divided by the geometric mean chord (c).

Thus, AR = b/c = b^2/bc = b^2/S.

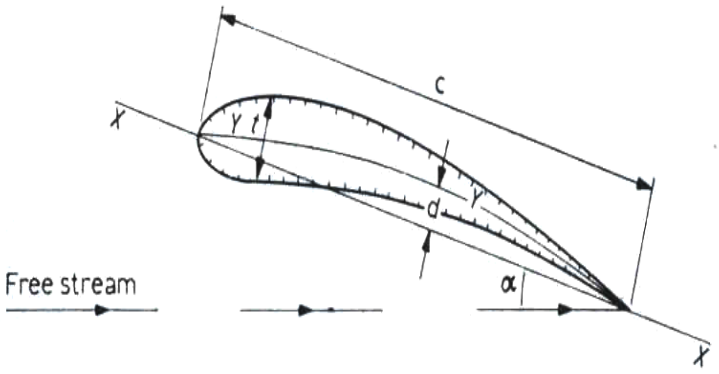

Figure 4: Aerofoil Terminology

Here, 'XX' is the Chord Line, 'c' means Chord Length, 't' is the Max Thickness, 'YY' indicates the Camber Line, 'α' specifies the Angle of Attack and 'd' is called the Max Camber.

There are various types of aerofoil like 4-digit, 5-digit, modified 4-/5-digit, 6-digit etc. There were many similarities between those airfoils but mainly two primary variables affect the shapes of an aerofoil which are the slope of the airfoil mean camber line and the thickness distribution above and below this line. These variations lead a series of equations to generate an entire family of related NACA airfoil shapes. 4-digit NACA 0015 symmetrical aerofoil profile and cambered aerofoil NACA 4415 of same volume have been chosen in this research work. The explanation of the 4-digit NACA 0015 and NACA 4415 aerofoil is as follows:

a. The first digit specifies the maximum camber in percentage of the chord. Abbott (1945) and Albert (1959)

b. The second digit indicates the position of the maximum camber in tenths of chord, Abbott (1945) and Albert (1959) and

c. The last two digits provide the maximum thickness of the airfoil in percentage of chord, Abbott (1945) and Albert (1959).

The thickness distribution above (+) and below (-) the mean line can be calculated by the following equation for each of the x-coordinates of 4-digit NACA symmetrical aerofoil [Abbott and Albert 1959]:

3. Experimental Design

Important features of experimental design of four major profiles, symmetric aerofoil NACA 0015, cambered aerofoil NACA 4415, cylinder and sphere are shown in the Table 1. Photograph of the four profiles are shown in the figures 5-8 respectively.

Table1: Important Features of Experimental Design of Four Profiles

	Experimental Features
NACA 0015 (Symmetric aerofoil)	Chord Length= 141.41mm and Span=240.7 Mm.
NACA 4415 (Cambered aerofoil)	Chord length=142.67 mm and Span= 247 mm.
Cylinder	Diameter= 38.72 mm, length=247 mm.
Sphere	Diameter= 90.8 mm.
Profile material	Wood (‘Gamary’)
Flow of air	Incompressible and subsonic
Air Speed (approximate), v	10 m/s, 15 m/s, 20 m/s, 25 m/s,
Air Density, ρ	1.17 $kg.m^{-3}$
Kinematic Viscosity, μ ($\times 10^{-5}$)	1.973 $kg.m^{-1}.s^{-1}$
Angle of Attack, α	-3˚ to 18˚ for the aerofoils with 3˚ steps 0˚ to 180˚ angles of the cylinder and sphere with 10˚ steps
Effect of temperature	Neglected

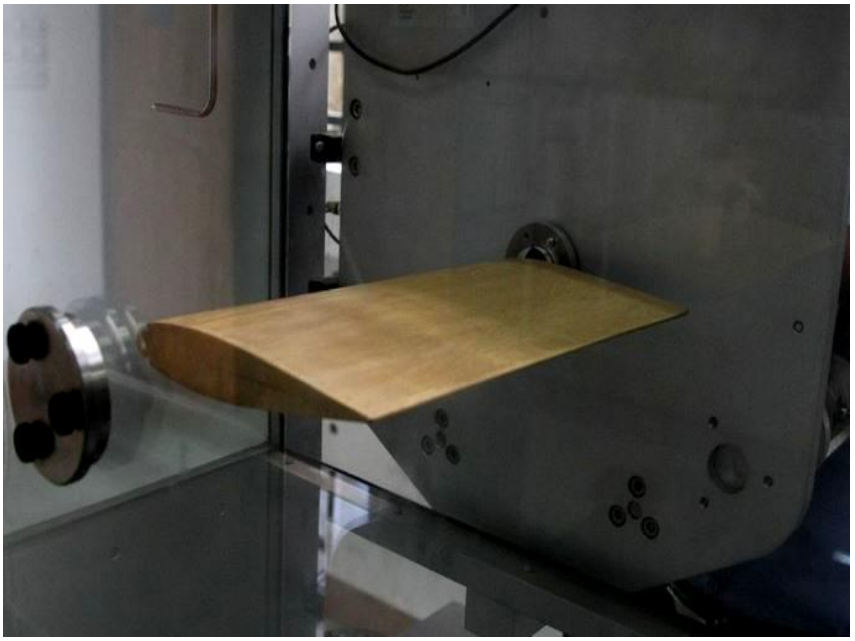

Figure 5: Photograph of Symmetrical Aerofoil (NACA 0015).

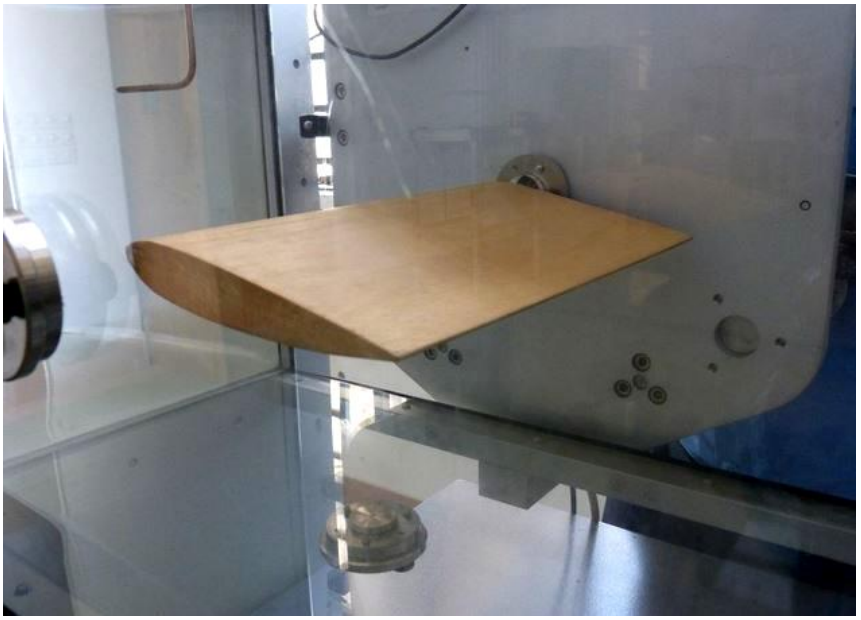

Figure 6: Photograph of Cambered Aerofoil (NACA 4415)

Figure 7: Photograph of Cylindrical Profile.

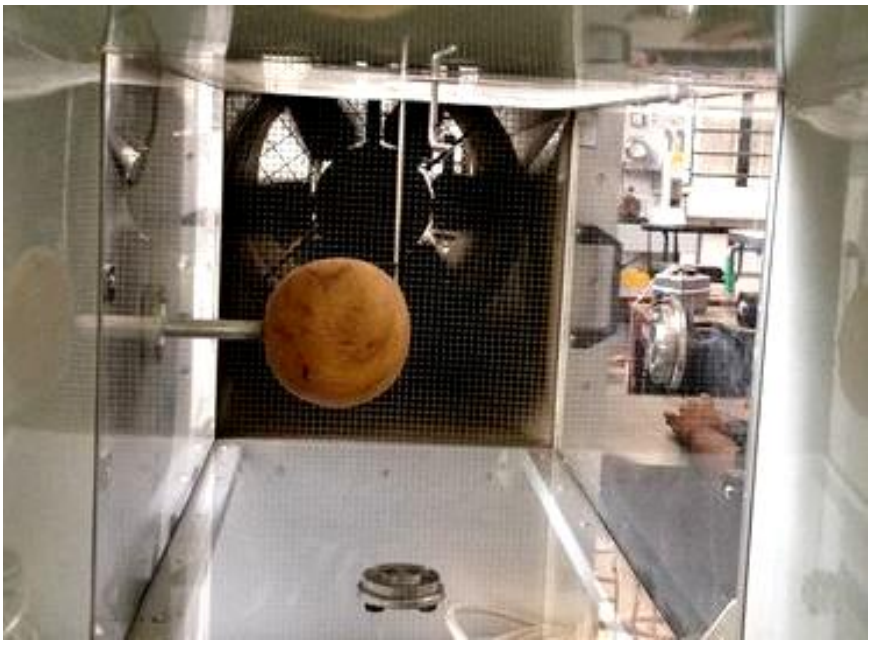

Figure 8: Photograph of Sphere Shaped Profile

4. Subsonic Wind Tunnel

Subsonic Wind Tunnel AF 100 has been used to test the fabricated profiles. The wind tunnel shown in figure 5 is a test bench used in aerodynamic research to study the effects of air moving past solid objects. It is a compact, practical open circuit suction wind tunnel for studying aerodynamic. Air enters the tunnel through an aerodynamically designed effuse that accelerate the air linearly to the working section, passes out through a grill, a diffuser and then to a variable speed axial fan. It has a working section of 300 mm by 300 mm and 600 mm long. The forces generated on the object by airflow have been measured with a sensitive three component balance shown in figure 6 and calculations of different values have been done by Versatile Data Acquisition System (VDAS).

Figure 9: Photograph of Subsonic Wind Tunnel AF 100.

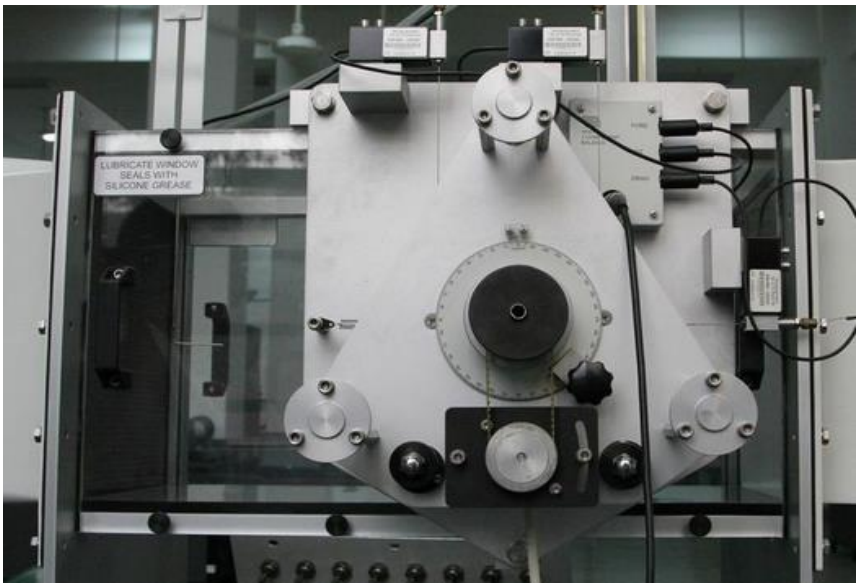

Figure 10: Working Section with Three Component Balance of Wind Tunnel.

5. Result and Discussion

5.1 Aerodynamic Characteristics of NACA 0015

The variation of drag coefficient with Reynolds number for symmetric aerofoil NACA 0015 is shown in following figure 11. The drag coefficient slightly decreases and gives a downward line with the increase of Reynolds number of the air for each angle of attack. Also it is found that with increasing angle of attack the values of drag coefficient increases respectively. After 12˚ AOA the drag coefficient increases suddenly high and shows a stall angle approximately at 14˚ AOA shown in figure 12.

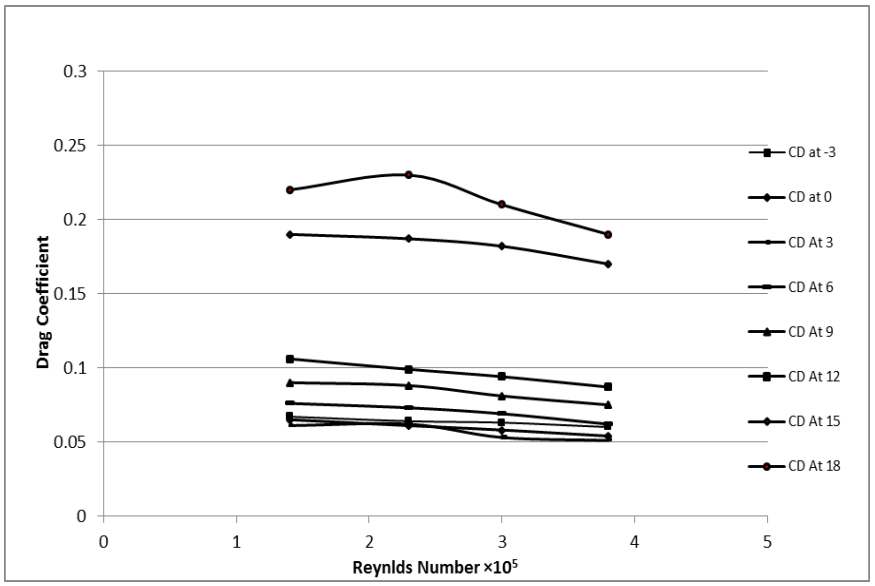

Figure 11: Drag Coefficient vs. Reynolds Number at Different Angle of Attack for NACA 0015.

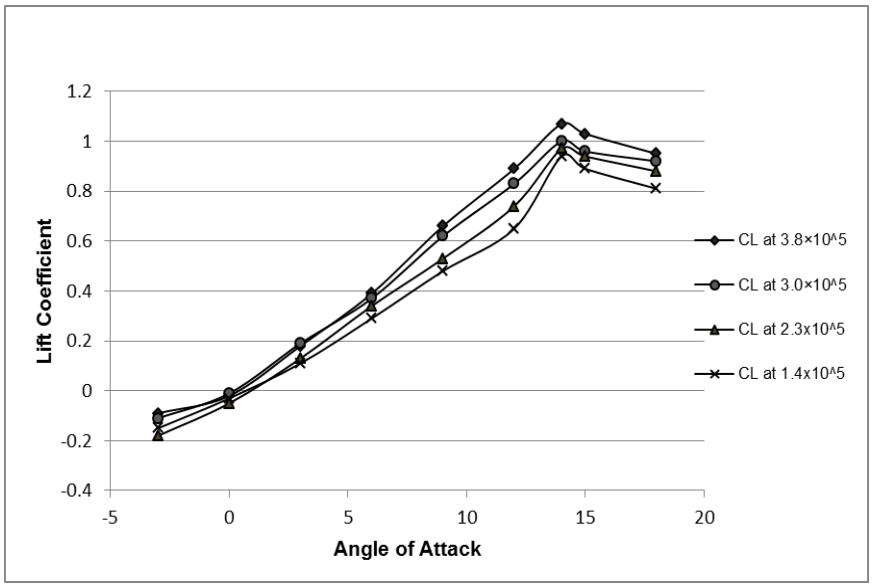

Figure 12: Variation of Lift Coefficient vs. Angle Of Attack at Different R_e Showing an Approx. Stall Angle at 14˚ AOA for NACA 0015.

5.2 Aerodynamic Characteristics of NACA 4415

The variation of drag coefficient with Reynolds number for cambered aerofoil (NACA 4415) is shown in following figure 13. The drag coefficient decreases a little and gives downward lines with the increase of Reynolds number of the air for each angle of attack. NACA 4415 gives less drag coefficient than NACA 0015. And NACA 4415 has a stall angle approximately at 16˚ AOA shown in figure 14, after which the drag coefficient increases rapidly.

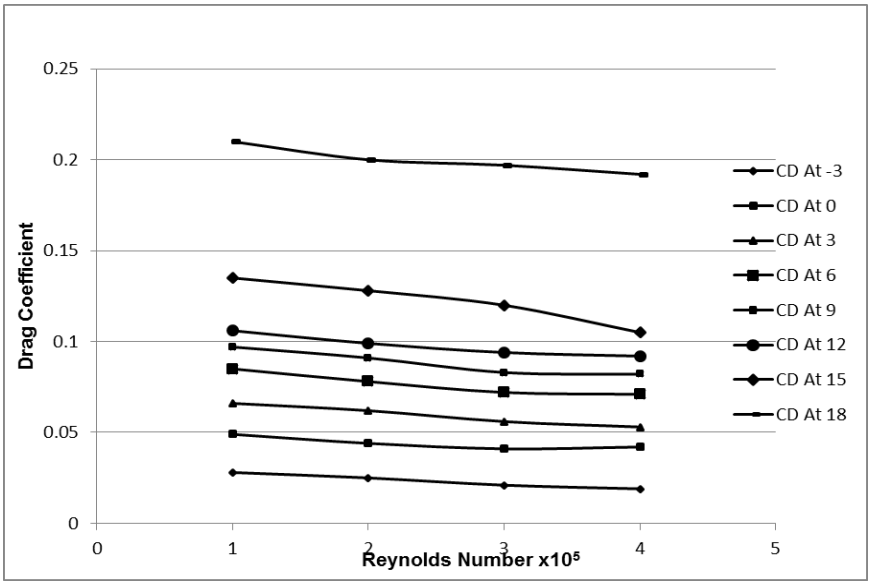

Figure 13: Drag Coefficient vs. Reynolds Number at Different Angle of Attack for NACA 4415.

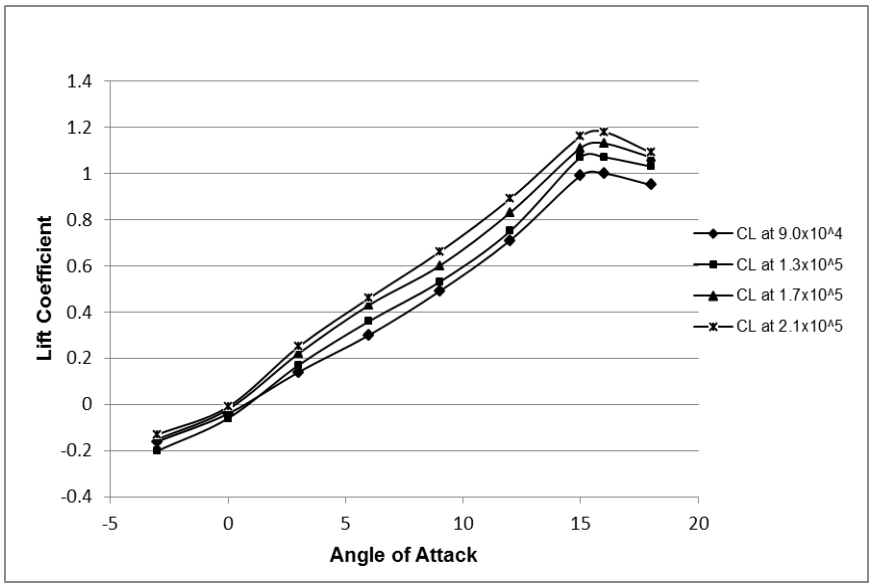

Figure 14: Variation of Lift Coefficient vs. Angle Of Attack at Different R_e Showing an Approx. Stall Angle at 16˚ AOA for NACA 4415.

5.3 Aerodynamic Characteristics of the Cylinder

The Drag Coefficient vs. Reynolds Number curves presented in figure 15 show a significant increase in Drag Coefficient with an increase in Reynolds number for cylinder. Theoretically in subsonic level of air speed the ideal curve is a straight line in this range of Reynolds number. The drag coefficient is approximately 1.2 [Scruton and Rogers, 1971] standard curve. But practically at low to high Reynolds number the Drag coefficient gradually rises and forms approximate constant line up to certain range of Reynolds number in the following.

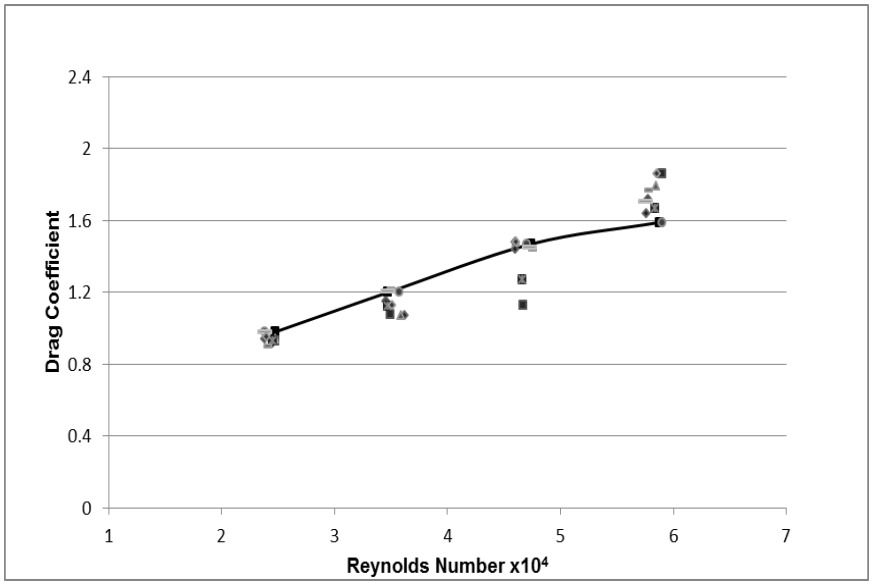

Figure 15: Drag Coefficient vs. Reynolds Number at Different Angular Position for the Cylinder.

5.4 Aerodynamic Characteristics of the Sphere

Theoretically the sphere in subsonic level of air speed shows a downward parabolic curve in the range of Reynolds number. The experiential drag coefficient vs. Reynolds number graph in figure 16 also gives a downward parabolic curve with the increase of Reynolds number. But the values of drag coefficient are higher than the ideal values for the geometry.

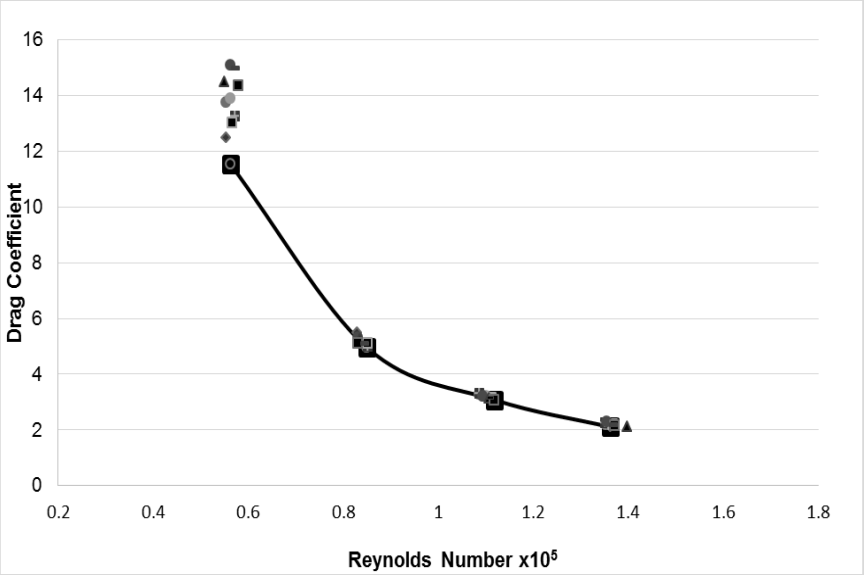

Figure 16: Drag Coefficient vs. Reynolds Number at Different Angular Position for the Sphere.

The difference between the four profiles drag coefficient is quite significant. The profile which has lesser drag coefficient, the more aerodynamic shape it is. From the investigation it has been observed that the cambered aerofoil NACA 4415 have less drag coefficient than symmetric aerofoil NACA 0015. For cylinder and sphere the cylinder has less drag coefficient than the sphere [Sheard, 2005]. And also the cylinder and sphere have much higher drag coefficient than the aerofoils. So firstly NACA 4415 and then NACA 0015 have better aerodynamic shape than the cylinder or sphere.

The Table 2 is made based on the difference between the drag coefficients of the cambered aerofoil NACA 4415 at 16˚stall angle, symmetric aerofoil NACA 0015 at 14˚ stall angle, cylinder and sphere at 10 m/s, 15 m/s, 20 m/s and 25 m/s air speed. The Table is given bellow:

Table 2: Comparison of Drag Coefficient of Four Profiles at Different Speed

Velocity	NACA 0015 (at stall angle)	NACA 4415 (at stall angle)	Cylinder	Sphere
10 m/s	0.136	0.134	0.92	11.53
15 m/s	0.129	0.127	1.26	4.96
20 m/s	0.120	0.117	1.46	3.08
25 m/s	0.105	0.103	1.78	2.1

From the above comparisons it is clear that the cambered aerofoil is distinctly the most efficient aerodynamic shape and the sphere is the less desired aerodynamic shape which highly disturbs the air flow.

6. Conclusion

The main objective of this thesis is the study of drag forces of different shaped profiles in different Reynolds number. The results obtained and the graph pattern seem to agree rather well with the experimental and theoretical, in particular on the drag coefficient vs. Reynolds number curves for examined cylinders, sphere, symmetrical aerofoil (NACA 0015) and cambered aerofoil (NACA 4415). Following this investigation; it was possible to put the light on the following points:

- With the increase of Reynolds number drag coefficient decrease respectively. The change pattern varies with the profile shapes. As the drag coefficient vs. Reynolds number curve for cylinder and sphere shows parabolic shape whereas the aerofoil shows almost linier decrement of drag coefficient with the increase of Reynolds number.
- The symmetrical aerofoil (NACA 0015) and cambered aerofoil (NACA 4415) gives low drag coefficient then the cylinder and sphere, so the aerofoils are the desired aerodynamic shape where high lift forces are required like airplanes, turbine blades etc.
- Fluid flow over it essentially follows the contours of the aerofoils, so it's said to be streamlined and a body that is not streamlined is said to be bluff. The fluid flow over a bluff body follows the contours of that body only part way, or not at all, so cylinder and sphere shape are bluff.
- The drag force over a cylinder or sphere is required for the design of the vehicles, builds shapes and also fuselage of the plane.

The importance of the experimental investigation is to clear up the physical phenomena described by the theory. And it has been found that the practically the physical phenomena and theory varies.

7. Recommendations

- The four profiles can be fabricated with even smooth surface material instead of wood to reduce surface friction drag and maintain its streamlines.
- The design and simulation of cylinder, sphere, symmetrical aerofoil (NACA 0015) and cambered aerofoil (NACA 4415) can also be done by Gambit and Fluent or other simulation software.
- In the experiment smoke can be used to visualize the streamline flow pattern of the air over the profiles.

References:

Clancy, L. J. (1975), "Aerodynamics", John Wiley, New York.

Anderson, J. D. (1991), "Fundamentals of Aerodynamics", McGraw-Hill Companies, 2nd edition.

Glauert, H. (1926), “The Elements of Aerofoil and Airscrew Theory”, Cambridge University Press, London.

Ladjedel, A. O., Yahiaoui, B. T., Adjlout, C. L. and Imine, D. O. (2011), “Experimental and Numerical Studies of Drag Reduction on a Circular Cylinder”, World *Academy of Science, Engineering and Technology, vol.*53, Pp.359

Sheard, G. J., Hourigan, K. and Thompson, M. C.,(2005) “Computations of the drag coefficients for low-Reynolds-number flow past rings”, J. Fluid Mech. (2005), vol. 526, Pp. 257–275..

Scruton, C., and Rogers, E. (1971) “Steady and unsteady wind loading of buildings and structures.” Philosophical Transactions of the Royal Society Vol. 269, Pp.353–383.